Phasorial differential pulse-width pair technique for long-range Brillouin optical time-domain analysis sensors

Javier Urricelqui, Mikel Sagues and Alayn Loayssa*

Departamento de Ingeniería Eléctrica y Electrónica,Universidad Pública de Navarra Campus Arrosadia s/n, 31006 Pamplona, Spain

alayn.loayssa@unavarra.es

Abstract: We introduce a novel phasorial differential pulse-width pair (PDPP) method for Brillouin optical time-domain analysis (BOTDA) sensors that combines spatial resolution enhancement with increased tolerance to non-local effects. It is based on the subtraction of the complex time-domain traces supplied by a sensor configuration that uses a phase-modulated probe wave and RF demodulation. The fundamentals of the technique are first described theoretically and using numerical simulation of the propagating waves. Then, proof-of-concept experiments demonstrate the measurement of the Brillouin frequency shift distribution over 50-km. The system is shown to withstand large variations of the pump power generated by its interaction with a powerful probe wave along the fiber; hence, highlighting the potential of the PDPP technique to increase the detected signal-to-noise ratio in long-range BOTDA. Moreover, the PDPP is also shown to increase the measurement contrast by allowing the use of relatively long duration pulses while retaining 1-m spatial resolution.

OCIS codes: (290.5900) Scattering, stimulated Brillouin; (060.2370) Fiber optics sensors; (040.2840) Heterodyne.

References and links

1. L. Thévenaz, S. F. Mafang, and J. Lin, "Effect of pulse depletion in a Brillouin optical time-domain analysis system," Opt. Express **21**(12), 14017–14035 (2013).
2. Y. Dong, L. Chen, and X. Bao, "System optimization of a long-range Brillouin-loss-based distributed fiber sensor," Appl. Opt. **49**(27), 5020–5025 (2010).
3. R. Bernini, A. Minardo, and L. Zeni, "Long-range distributed Brillouin fiber sensors by use of an unbalanced double sideband probe," Opt. Express **19**(24), 23845–23856 (2011).
4. A. Minardo, R. Bernini, L. Zeni, L. Thévenaz, and F. Briffod, "A reconstruction technique for long-range stimulated Brillouin scattering distributed fibre-optic sensors: Experimental results," Meas. Sci. Technol. **16**(4), 900–908 (2005).
5. W. Li, X. Bao, Y. Li, and L. Chen, "Differential pulse-width pair BOTDA for high spatial resolution sensing," Opt. Express **16**(26), 21616–21625 (2008).
6. K. Y. Song, S. Chin, N. Primerov, and L. Thévenaz, "Time-domain distributed fiber sensor with 1 cm spatial resolution based on Brillouin dynamic grating," J. Lightwave Technol. **28**(14), 2062–2067 (2010).
7. A. Motil, O. Danon, Y. Peled, and M. Tur, "High spatial resolution BOTDA using simultaneously launched gain and loss pump pulses," Proc. SPIE **8794**, 87943L (2013).
8. J. Urricelqui, A. Zornoza, M. Sagues, and A. Loayssa, "Dynamic BOTDA measurements based on Brillouin phase-shift and RF demodulation," Opt. Express **20**(24), 26942–26949 (2012).
9. J. Urricelqui, M. Sagues, and A. Loayssa, "BOTDA measurements tolerant to non-local effects by using a phase-modulated probe wave and RF demodulation," Opt. Express **21**(14), 17186–17194 (2013).
10. A. R. Charaplyvy, R. W. Tkach, L. L. Buhl, and R. C. Alferness, "Phase modulation to amplitude modulation conversion of CW laser light in optical fibres," Electron. Lett. **22**(8), 409–411 (1986).
11. C. L. Tang, "Saturation and spectral characteristics of the Stokes emission in the stimulated Brillouin process," J. Appl. Phys. **37**(8), 2945–2955 (1966).
12. S. Foaleng-Mafang, J. Beugnot, and L. Thevenaz, "Optical sampling technique applied to high resolution distributed fibre sensors," Proc. SPIE **7503**, 750369 (2009).

#208931 - $15.00 USD Received 25 Mar 2014; revised 5 May 2014; accepted 5 May 2014; published 10 Jul 2014

1. Introduction

Brillouin optical time-domain analysis (BOTDA) sensors are bound to become a fundamental tool for monitoring in a number of industries ranging from civil engineering to oil and gas pipelines or electric power. This wide variety of applications is stimulating a very important research effort into these sensors. One of the main trends is the development of long-range BOTDA sensors, where the ultimate distance is constrained by several effects including the so-called non-local effects. These are caused by the continuous transfer of energy between the probe and pump waves along the fiber, which modifies the pump power by introducing a wavelength dependence that leads to errors in the Brillouin frequency shift (BFS) measurements [1]. This is a major limitation that constricts the maximum power of probe wave that can be injected in the sensing fiber and hence the signal to noise ratio (SNR) of the detected signal. Therefore, several countermeasures have been proposed [1–4].

Another key challenge in BOTDA sensors is to enhance the spatial resolution of the measurements in order to increase the number of resolved points along the optical fiber. The spatial resolution is directly related to the pump pulse length. However, decreasing the temporal duration of the pump pulses to enhance the spatial resolution has a negative impact on the Brillouin frequency shift (BFS) measurement precision because it leads to Brillouin line-width broadening [5]. There are different proposals to overcome this limitation [5–7]. However, one of the most effective and easy to deploy in long-range BOTDA sensors is the differential pulse width pair (DPP) technique [5], which is based on the subtraction of the time domain Brillouin signals measured by sequentially injecting two pump pulses with slightly different pulse durations. This enhances the spatial resolution of the measurement, which is given by the pulse-width difference, and simultaneously preserves the BFS precision, as the Brillouin line-width is defined by the comparatively long duration of the individual pulses.

In this paper, we introduce a novel phasorial differential pulse-width pair (PDPP) technique that provides tolerance to non-local effects in addition to enhancement of the spatial resolution. It is derived from a BOTDA scheme that we have recently proposed, which uses a phase-modulated probe wave and RF demodulation to give measurements largely immune to changes of the pump pulse power [8,9]. The method takes advantage of the complex signals (magnitude and phase-shift) supplied by this system to perform a full phasorial subtraction of the responses to two sequential pump pulses with differential duration.

2. Fundamentals

The principle of the proposed technique is based on a BOTDA sensor that uses a probe wave obtained by modulating the phase of an optical carrier with an RF tone in an electro-optic phase modulator [9]. The first upper-sideband of the modulation is used as probe wave for the stimulated Brillouin scattering (SBS) generated by a counter-propagating pump pulse. This induces a slight variation to its optical field, modifying the amplitude and phase-shift with a transfer function given by the complex Brillouin spectrum. The resulting modulated wave is detected and RF demodulated giving rise to an RF signal (magnitude and phase-shift) that can be expressed for a given location of a long sensing fiber, z, as [9]:

$$I(z) \approx 2E_0E_{SB}\frac{\cos(\phi)g_0\Delta\nu_B}{\sqrt{\Delta\nu_B{}^2+4\Delta\nu^2}}\exp\left[-j\arctan\left(2\frac{\Delta\nu}{\Delta\nu_B}\right)\right]+$$
$$+2E_0E_{SB}\sin(\phi)\exp(-j\pi/2)\left[1+\exp\left(\frac{g_0\Delta\nu_B}{\Delta\nu_B+j2\Delta\nu}\right)\right] \quad (1)$$

where E_0 and E_{SB} are, respectively, the amplitudes of the optical fields of the carrier and sidebands of the phase-modulated probe wave (higher-order sidebands were neglected, assuming a small modulation index), g_0 is the local Brillouin gain, $\Delta\nu_B$ is the Brillouin line-width, $\Delta\nu=\nu-\nu_P+\nu_B(z)$ is the detuning of the interaction frequency from the center of the

#208931 - $15.00 USD Received 25 Mar 2014; revised 5 May 2014; accepted 5 May 2014; published 10 Jul 2014

Brillouin spectrum, v_P is the optical frequency of the pump wave, v_B is the Brillouin frequency shift at position z and ϕ is the relative phase difference between carrier and sidebands caused by chromatic dispersion at the fiber [10]:

$$\phi = \frac{L\pi cDf_{RF}^{\ 2}}{v_0^{\ 2}} \tag{2}$$

where L is the length of the fiber, c is the velocity of light in free space, D is the fiber dispersion parameter, v_0 is the optical frequency of the carrier and f_{RF} is the modulation frequency. Compared to our previous works [8,9], Eq. (1) incorporates the well-known effect of phase to intensity modulation conversion through chromatic dispersion in long fibers [10]. This is clearly shown in Eq. (1), where the first term on the right-hand side is the detected phasor originated by SBS interaction with a phase-modulated wave and the second term is that originated using an intensity-modulated wave. Considering that we have small chromatic dispersion or that it is compensated making $\phi \gg 0$, the detected RF signal is then given by the first term of Eq. (1), whose RF phase-shift signal has no dependence with the particular local Brillouin gain associated to the SBS process. As a consequence, it does not depend on the pump power. This has major implications, as RF phase-shift based measurements are not going to be affected by non-local effects because they are independent of the frequency dependent changes of the pump pulse power [9]. Therefore, a higher probe wave power can be used to enhance the SNR or to achieve larger monitoring distances.

The signal detected in Eq. (1) is deployed in a novel PDPP scheme where instead of simply subtracting two consecutive time domain BOTDA traces to obtain the differential magnitude signal, we perform a full phasor subtraction of the complex responses (magnitude and phase-shift) obtained by sequentially injecting two pulses with different duration. This process is illustrated in Fig. 1 that schematically depicts the measurement at location z_0 of a fiber section that has a given BFS (BFS_1) followed by a short section with a different BFS (BFS_2). A first pulse with a spatial length of u is injected in the fiber, yielding, for the measurement at location z_0, an RF signal represented by phasor I_1. This resultant RF signal is affected by the integrated Brillouin gain and phase-shift (characterized by BFS_1) experienced by the probe wave over the length covered by this first pulse. Then, a second pump pulse of differential duration (Δu) is injected and the RF signal measured for the same location will be affected by the complex Brillouin spectra of both consecutive fiber sections (characterized by BFS_1 and BFS_2), leading to a change in the amplitude and phase-shift of a second phasor I_2 that represents this second RF signal. Finally, the two phasors are subtracted to obtain the differential RF signal, which corresponds to the Brillouin interaction in the differential length Δu (characterized by BFS_2). Therefore, enhanced spatial resolution is obtained. Moreover, the RF phase-shift, $\Delta\theta_{RF}$, of this differential signal retains the tolerance to non-local effects described above.

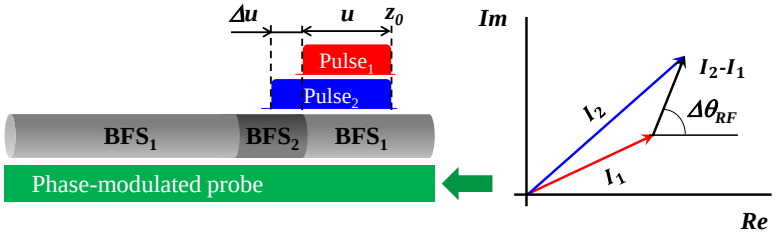

Fig. 1. Schematic representation of SBS interaction and the received RF signal using the PDPP technique.

The scenario described above has been analyzed by numerically solving the coupled ordinary differential equation system that gives the evolution of the optical fields of the probe E_S and pump waves, E_P, along the fiber [11]:

#208931 - $15.00 USD Received 25 Mar 2014; revised 5 May 2014; accepted 5 May 2014; published 10 Jul 2014

$$\frac{dE_S(z)}{dz} = \left[\frac{jg_0\Delta\nu_B}{\left(\Delta\nu - j\left(\Delta\nu_B/2\right)\right)}\left|E_P\right|^2 + \frac{\alpha}{2}\right]E_S \tag{3.a}$$

$$\frac{dE_P(z)}{dz} = \left[\frac{-jg_0\Delta\nu_B}{\left(\Delta\nu + j\left(\Delta\nu_B/2\right)\right)}\left|E_S\right|^2 - \frac{\alpha}{2}\right]E_P \tag{3.b}$$

where α is the fiber attenuation. The solution of these equations gives the optical field of the upper-sideband of the modulated wave, while the carrier and lower-sideband are assumed to only attenuate along its propagation. Moreover, the calculations are simplified assuming steady-state conditions for long pulse lengths of 5 m and 6 m.

Figure 2(a) shows the RF magnitude and phase-shift spectra at position, z_0, for each pump pulse and the resulting differential RF spectra. Notice that the calculated spectra using a 6 m pulse length clearly display the combined response to the two consecutive fiber sections with different BFS, while the magnitude and phase-shift of the differential phasor signal just retains the response to the second section (BFS_2), as expected. Therefore, the proposed technique presents an enhanced spatial resolution and BFS accuracy in RF magnitude and phase-shift measurements.

Furthermore, it has also been found that the differential RF phase-shift signal keeps the same properties regarding non-local effects than the individual responses to each pulse. Figure 2(b) presents the calculated differential RF spectra for several probe powers considering the worst case situation for non-local effects, which occurs when the BFS_2 has a frequency difference of $\Delta\nu_B/3$ with the rest of a uniform BFS fiber [1]. In these simulations, the peak of the magnitude spectra are clearly biased from the real BFS measurement for increasing probe power, meanwhile the differential RF phase-shift spectra remains unaltered. A loss-based BOTDA is assumed in these calculations, but the distortion induced to the measured spectra is independent of the sensor's configuration (loss or gain), the only difference resides in the direction of the Brillouin spectrum biasing.

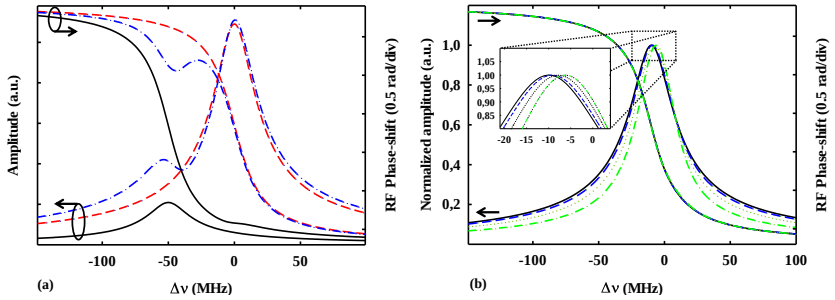

Fig. 2. (a) Calculated magnitude and RF phase-shift spectra for 5m (red-dashed line), 6m (blue-dot-dashed line) pulse lengths and the differential RF spectra (black-solid line) for a BFS difference of 50MHz between sections. (b) Calculated magnitude and RF phase-shift spectra for a BFS difference of 10 MHz and different injected probe powers: 20μW (black-solid line), 45μW (blue-dashed line), 100μW (red-dotted line) and 200μW (green-dot-dashed line). Simulations parameters are $g_0 = -1.5\ 10^{-11}$m/W, $\Delta\nu_B = 30$ MHz, L = 30 km, effective area is $7.18\ 10^{-11}$m^2 and the injected optical pump power is 100mW.

3. Experimental setup and measurements

The experimental setup sketched in Fig. 3 was assembled in order to evaluate the potential of the technique. The light from a distributed feedback (DFB) laser diode at 1560 nm is coupled into two optical branches. In the upper branch, a double-sideband suppressed-carrier modulation is generated using a Mach-Zehnder electro-optic modulator (MZ-EOM) driven by a microwave tone whose frequency is tuned around 9.5 GHz. The resultant signal is pulsed using a semiconductor optical amplifier (SOA) and then amplified by an erbium-doped fiber

#208931 - $15.00 USD Received 25 Mar 2014; revised 5 May 2014; accepted 5 May 2014; published 10 Jul 2014

amplifier (EDFA). The upper-sideband of the pulsed signal is selected using a narrowband fiber Bragg grating (FBG) obtaining the desired pump wave. Its state of polarization is randomized with a polarization scrambler to reduce polarization-mismatching-induced fluctuations on the signal before being launched into the sensing fiber via a circulator. In the lower branch, a probe wave is generated with an electro-optic phase modulator driven by a 1.3 GHz RF signal. Once the probe wave has interacted with the pump pulse via SBS, the chromatic dispersion phase-shift is corrected using a dispersion compensating module (DCM) prior to signal detection. Finally, the resultant RF signal is demodulated and captured in a digital oscilloscope. The deployed RF demodulator's bandwidth is 220MHz, so that changes faster than 10ns in the demodulated signal can be resolved (1 m resolution). For higher spatial resolutions, the needed bandwidth should be adjusted to 1.5/τ, where τ is the pulse duration [12]. Note that for the low f_{RF} used in this setup, the sensing fiber length needed to completely convert the phase modulation into an intensity modulation is around 2000 km. For the deployed 50-km-long fiber, chromatic dispersion only induces a slight phase-shift at the sidebands, which has no real impact in the measurements because the second term in Eq. (1) becomes merely a DC baseline. The DCM was simply used to reduce this DC in order to fully exploit the dynamic range of the RF demodulator and oscilloscope.

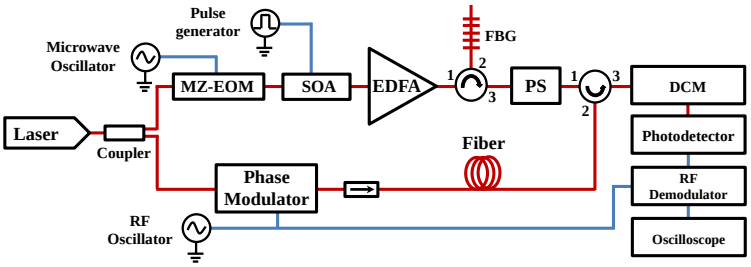

Fig. 3. Experimental setup for the PDPP-BOTDA sensor based on phase-modulated probe wave and RF demodulation.

In order to evaluate the detrimental impact of non-local effects in long-range measurements, the probe wave power is set to a value, 0.54 mW, that clearly outreaches the maximum power (45 μW), at which this effect becomes more serious [1]. This huge optical power results in amplification of the pump pulse power due to the energy transfer from the probe wave to the pump pulse in a loss-based BOTDA sensor. Figure 4(a) shows this effect, where the optical power of the pump pulse is amplified to more than double its original value (a factor of 115%) for the frequency difference between both waves that matches the average BFS of the optical fiber (set as $\Delta\nu = 0$). This value largely exceeds the maximum tolerable factor (17%), which induces a measurement error of 1 MHz at the worst case scenario, where a long fiber with a uniform BFS is followed by a small section at the end of the fiber with a BFS change [1].

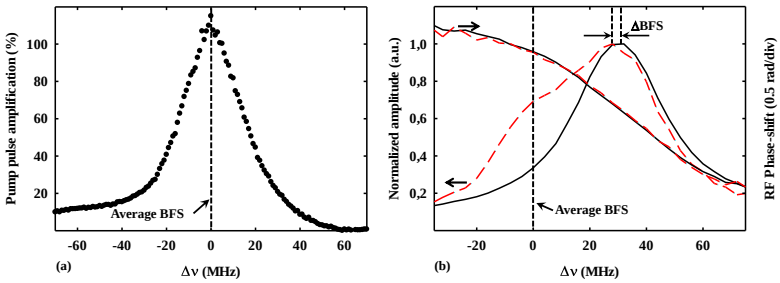

Fig. 4. (a) Measured pump pulse amplification at the end of the fiber. (b) Measured amplitude and RF phase-shift spectra at the hot spot section when that section is located at the probe input (red-dashed line) or at the pump input (black-solid line).

#208931 - $15.00 USD Received 25 Mar 2014; revised 5 May 2014; accepted 5 May 2014; published 10 Jul 2014

Such scenario was simulated by inserting a 13-m length section at the end of the fiber in a climatic chamber at 61°C. Figure 4(b) depicts the amplitude and RF phase-shift spectra for that section, using 50 ns pump pulses for two measurements performed by swapping the fiber input ends of pump and probe waves, which is an effective method to observe the influence of non-local effects [2]. Notice that when the hot spot is located at the probe end of the fiber, the amplitude spectrum is distorted and there is a biasing effect that introduces a measurement error. In contrast to the amplitude spectra, the shape of the RF phase-shift spectra remains unaltered for both measurements.

A similar experiment was performed but, this time, deploying the full phasor subtraction of the time-domain BOTDA traces measured by sequentially injecting two pump pulses of 50 and 60 ns. The experimental results shown in Fig. 5(a), match those obtained using 50 ns pulses, apart from the expected reduction of SNR due to the enhanced spatial resolution. The precision achieved in the BFS measurements based on RF phase-shift was 1.3 MHz (1.3°C/26 με) at the worst contrast position. Finally, in order to demonstrate the spatial resolution enhancement, one meter was extracted from the final section located at the climatic chamber and placed at room temperature in a loose state. Figure 5(b) depicts the color coded RF phase-shift distribution along the final section of the fiber. At the location corresponding to the room temperature one-meter section, a shift from $\Delta\nu$ ~30 MHz to ~-5 MHz, which fits the temperature change for that section, is clearly appreciable.

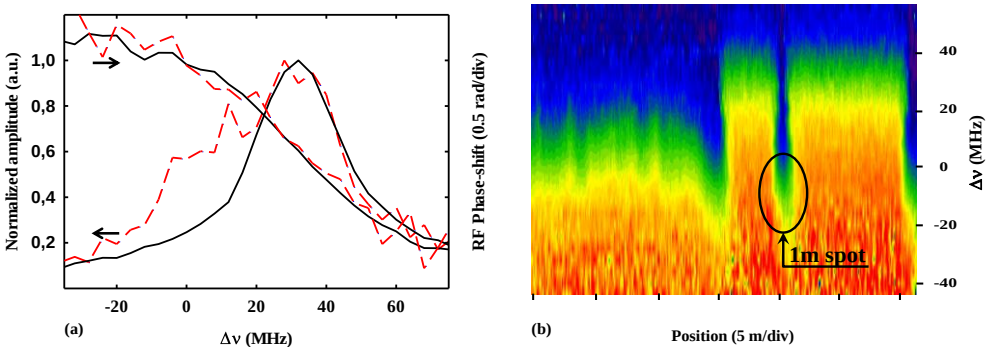

Fig. 5. (a) Differential amplitude and RF phase-shift spectra at the hot spot section, when that section is located at the probe input (red dashed line) or at the pump input (black solid line). (b) Differential RF phase-shift distribution.

4. Conclusions

In this work, we have presented a long-range BOTDA sensor that merges the advantages of the DPP technique and the deployment of a phase-modulated probe wave and RF demodulation. The former provides RF phase-shift measurements with high spatial and spectral resolution and the latter gives rise to RF phase-shift spectra that have no dependence with the apparition of non-local effects. Therefore, two of the fundamental drawbacks of the conventional long-range BOTDA can be overcome. Finally, an experimental proof-of-concept has been performed with a 50-km-long fiber, obtaining unaltered phase-shift spectra in presence of non-local effects. Moreover, a 1-m section has been detected by using the RF phase-shift of the differential Brillouin signal.

Acknowledgments

The authors wish to acknowledge the financial support from the Spanish Ministerio de Ciencia e Innovación through the project TEC2010-20224-C02-01 and from the Universidad Pública de Navarra.

#208931 - $15.00 USD Received 25 Mar 2014; revised 5 May 2014; accepted 5 May 2014; published 10 Jul 2014